Metallophores associated with *Trichodesmium erythraeum* colonies from the Gulf of Aqaba

Martha Gledhill,*[a] Subhajit Basu[b,c] and Yeala Shaked[b,c]

Trichodesmium **is a globally important marine nitrogen fixing cyanobacteria which forms colonies and utilizes atmospherically derived dust as a source for the limiting micro-nutrient iron. Here we report the identification of metallophores isolated from incubations of natural *Trichodesmium* colonies collected from the Gulf of Aqaba in the Red Sea. Three of our compounds were identified as the ferrioxamine siderophores B, E, and G. The remaining fifteen metallophores had mass to charge ratios that, to our knowledge, are not common to known siderophores. Putative sum formulas suggest most of these compounds were not structurally related to each other. We also found that the novel metallophores readily formed complexes with aluminium and were less specific for iron than the ferrioxamines. In our incubations of *Trichodesmium* colonies, the abundance of ten of the novel metallophores positively correlated with *Trichodesmium* biomass, but not with bacterial biomass, whilst ferrioxamine siderophores were more strongly associated with bacterial biomass. We identified ferrioxamines and our novel metallophores in filtered surface seawater samples from the Gulf of Aqaba. However, our novel metallophores were only observed in the surface seawater sample collected at the time of highest *Trichodesmium* abundance, while ferrioxamines were observed even when *Trichodesmium* was not present. We hypothesize that the novel metallophores were specifically associated with *Trichodesmium* colonies. Together with the bacterially produced ferrioxamines they likely contribute to a distinctive "ligandosphere" surrounding the *Trichodesmium* colonies, with potential implications for metal homeostasis within the colony environment.**

Introduction

Trichodesmium sp. occur throughout the tropical oligotrophic surface ocean, make a significant contribution to the supply of new nitrogen to the surface waters[1,2], and are key players in determining the balance in the nitrogen budget of the world's ocean[1,3]. *Trichodesmium* has a high requirement for the essential micro-nutrient iron (Fe)[4], which is typically present at very low concentrations (<0.2 nmol L^{-1}) in open ocean surface waters[5]. *Trichodesmium* is thought to adopt a number of strategies that include exploitation of Fe derived from atmospheric dust and optimisation of nitrogen fixation and photosynthesis in order to obtain and efficiently utilise Fe in the open ocean[6–8]. Maintenance of photosynthesis at the cost of nitrogen fixation (diazotrophy)[7], has been shown to reduce Fe requirements and thus may allow *Trichodesmium* to survive even long term periods of Fe limitation. However, since such strategies are typically associated with a reduction in nitrogen fixation, they have the potential to negatively impact on the ability of *Trichodesmium* to occupy its critical diazotrophic niche within a mixed community.

Exploitation of nutrient pools with more limited bioavailability, such as mineral or colloidal Fe[6], likely extends the geographical range of *Trichodesmium* and allows it to successfully exploit ecological niches that are nitrogen limited, but have a supply of mineral Fe from e.g. atmospheric dust deposition[9,10]. *Trichodesmium* has been shown to actively acquire and shuttle mineral dust to the centre of colonies[6], and colloidal Fe has been shown to be taken up by *Trichodesmium*[11]. Thus, an ability to move particles within a *Trichodesmium* colony allows for exploitation of Fe from mineral particles[6]. However, the mechanism by which Fe is mobilized from dust is not fully understood. Likely multiple pathways exist that include reductive dissolution and ligand assisted dissolution of Fe from particles. Reductive dissolution can occur within the colony via transient increases in reductive potential[12]. Furthermore, colonies foster a cohort of associated microbes with potential for mutualistic interactions[13,14] and consequent increased metabolic potential for exploitation of dust derived minerals[15]. *Trichodesmium* colonies thus provide a unique habitat within which mineral Fe can be solubilised by heterotrophic bacteria via production of ferrioxamine siderophores[15] and thereby made available to both *Trichodesmium* and its microbial consortium in a potential Fe-for-carbon and/or nitrogen (C/N) trade off[16]. Such strategies likely contribute to a higher abundance of *Trichodesmium* observed in regions receiving enhanced atmospheric Fe inputs from desert dust, such as the tropical North Atlantic, South China Sea and Red Sea/Gulf of Aqaba[3].

We have shown that heterotrophic bacteria within the *Trichodesmium* colony environment can produce ferrioxamine siderophores[17], confirming molecular evidence suggesting siderophore production by colony consortia[13,14]. However, *Trichodesmium* colony consortia also produce exopolymeric substances (EPS), with increased production observed under Fe stress and during bloom termination[18,19]. Since EPS also impact Fe biogeochemistry[20,21], it is possible that further unknown metallophores are present within the complex EPS-rich environment of the *Trichodesmium* colony and that these metallophores play a role in ligand assisted dissolution of iron minerals.

Here we use metal isotope profiling (MIP) to identify novel high affinity Fe-binding compounds associated with *Trichodesmium* colonies. Metal isotope profiling is being increasingly applied to the identification of siderophores and other metallophores in natural samples and cultures[22–25], where low metallophore abundance restricts the utility of more traditional assay approaches. MIP incorporates software driven mining of high resolution electrospray ionisation mass spectra to identify metallophores from the distinct isotopic signatures of the metal complexes[23,24,26–28]. The sensitivity of the method is enhanced either via enrichment with stable isotopes, via metallophore binding with metals with distinctive natural isotopic ratios[22,29]

or via combination with a metal specific detection method such as inductively coupled plasma mass spectrometry[25]. These approaches have shown that extensive suites of metallophores can be present in the marine[26,30–32] and other environments[33–37].

We applied MIP to extracted supernatants of incubated *Trichodesmium* colonies in order to identify unknown metallophores associated with the colony consortia. Natural *Trichodesmium* tuft-shaped colonies were collected from the Gulf of Aqaba (GoA) on four separate occasions in 2016 and 2017 and incubated over 1 to 3 days. Supernatant extracts were screened for Fe binding metallophores by exchanging Fe for gallium (Ga), which has a distinctive isotopic signature and thus facilitates siderophore identification[22]. We characterised detected metallophores using predicted sum formulas, hydrophobicity and relative affinity for aluminium (Al) a competing trivalent metal ion, which is often present at higher concentrations than iron in the marine environment[38]. We investigated the relationship between the relative abundance of the metallophores, *Trichodesmium* and associated bacteria in an effort to decipher the source of the metallophores. Furthermore, we added atmospherically derived dust sourced from the Gulf of Aqaba[39] to our colonies to assess the influence of this potential source of mineral Fe on the abundance of metallophores in incubations. We hypothesized that addition of an Fe source of low natural bioavailability would increase production of metallophores, particularly siderophores[17]. Finally, we screened surface seawater sampled from the GoA at times of high and low *Trichodesmium* abundance to assess if these novel metallophores have the potential to influence bulk seawater Fe biogeochemistry in regions that experience *Trichodesmium* blooms.

Experimental

Reagents

High purity water (18.2 mΩ cm^{-1}, Millipore) was used throughout. Incubation flasks were made from polycarbonate (1 L, Nalgene, Thermo Scientific) and were acid washed in 0.1 mol L^{-1} hydrochloric acid and microwave sterilised[40] prior to use. All sample handling and manipulations were performed under high efficiency particle air filters in order to minimise metal and microbial contamination (HEPA laminar flow hood). Metallophores were extracted from solution using 200 mg hydroxylated polystyrene-divinylbenzene solid-phase extraction (SPE) cartridges (3 mL, 90 µm particle size, 800 Å pore diameter, Isolute ENV+, Biotage). All solvents were of liquid-chromatography – mass spectrometry grade (Optima, Thermo). Metals for isotope profiling were obtained as single element standards in nitric acid (0.3 mol L^{-1} HNO_3, Inorganic Ventures). Other reagents were purchased from Thermo Scientific, except where otherwise stated.

Incubations of natural *Trichodesmium* colonies

Trichodesmium colonies were sampled from the pier at the Inter-University Institute, Eilat on April 20th (GoA-1), May 1st (GoA-2a) and May 2nd (GoA-2b) in 2016 and on May 7th (GoA-3) in 2017. Samples were collected when *Trichodesmium* was observed in high abundance (i.e. as a bloom) at the sea surface (Fig. S1a). *Trichodesmium* blooms were formed during a calm sea-state (Table S2) but dissipated rapidly with a change in wind or tide, so that the surface presence of blooms was typically ephemeral and lasted only 20-30 minutes. The blooms typically occurred as pronounced stratification developed in the GoA following winter mixing.

The *Trichodesmium* colonies were scooped into acid-cleaned wide mouthed 20 L high density polyethylene plastic containers, which were capped immediately after sampling. Sampling in such a manner helped us to gather a high biomass of colonies needed for metallophore detection, whilst minimising colony disruption. However, the transient nature of the blooms restricted replication of treatments for all but one experiment (May 2017, n=2). To overcome the lack of biological replication within experiments, we repeated our experiments on four separate occasions.

Colonies were hand-picked with a plastic dropping pipette into a petri-dish filled with filtered (0.2 µm), sterilized seawater (400 W microwave, 15 minutes, FSW). Morphological examination of the samples under stereoscope showed that colonies were dominated by needle shaped tufts of *Trichodesmium erythraeum* colonies (Fig. S1). Colonies were resuspended in 500 mL filtered seawater (FSW) in incubation flasks. Once all colonies had been added to the FSW, the flasks were gently mixed. One flask was sacrificed for detection of metallophores at the initial time point. For GoA-1, three further flasks were prepared. One was incubated for 24 hours following resuspension. After 24 hours, atmospherically derived mineral dust known to contain ca. 2 mg g^{-1} of Fe and ca. 3 mg g^{-1} Al in the acetic acid leachable fraction[39] was added to another flask at a concentration of 1 mg dust L^{-1}, whilst the remaining flask was left as a control. The flasks were then incubated under 100 µmol m^{-2} sec^{-1} light (12:12 hr photoperiod) at 25°C for a further 48 hours before filtration and extraction of siderophores. For further experiments, dust was added to one or two flasks immediately after resuspension, with a further one or two flasks left as controls, and incubations were kept to 24 hours. For each incubation set, ca. 5 ml was preserved with 2% glutaraldehyde (v/v) for determination of bacteria and trichome concentrations at initial and final time points. To count bacteria, 2ml of preserved sample was vortexed to disrupt *Trichodesmium* colonies, stained with 4',6-diamino-2-phenylindole and filtered on a black 0.22 µm polycarbonate filter (Whatman). Filters mounted on slides were imaged at 100× using a Nikon Eclipse-Ci epifluorescent microscope. Trichome counts were conducted using a Sedgewick-Rafter Cell (Pyser-SGI) under bright-field, using 10-20× magnification[11].

Preconcentration and analysis of metallophores

Approximately 500 mL of incubated seawater was filtered (0.2 µm, 25 mm PVDF sterile syringe filters, Millex®GV) and pumped over the SPE cartridge using a peristaltic pump at ambient seawater pH (~8), at a flow rate of approximately 3-5 mL min^{-1}.

After preconcentration, cartridges were flushed with air and frozen at -20 °C prior to shipment to GEOMAR. Once defrosted, cartridges were washed with 5 mL 10 mmol L^{-1} $(NH_4)_2CO_3$ adjusted to pH 8 – 8.3 by addition of formic acid. Metallophores were then eluted with 5 mL 81:14:5:1 (vol:vol:vol:vol) acetonitrile: propan-2-ol: H_2O: formic acid[30]. A 2 mL aliquot was then evaporated to ca. 150 µL and diluted with 600 µL 0.1 % formic acid. We used a low pH (ca. 2.5) in the final solution because our study focused on high affinity metallophores. Weights were recorded at each extraction and evaporation step to allow for determination of a preconcentration factor, given a density of 0.9 g mL^{-1} for the elution solvent at room temperature (21°C). Matrix effects and recovery efficiencies were not accounted for, with previous work suggesting a recovery efficiency of ca. 40% for ferrioxamine B[30]. Each sample was split into 6 × 100 µL aliquots. Aliquot #1 was analysed directly. 5 µL of a 10,000 mg
L^{-1} solution of Ga was added to aliquot #2, 5 µL 0.01 M freshly made $FeCl_3$ was added to aliquots #3, #4 and #5 and 10 µL 1,000 mg L^{-1} Al added to aliquot #6. All aliquots with metal additions were allowed to equilibrate overnight. The following day, further additions of ferrioxamines B (Sigma), G and E (EMC Microcollections) were made to aliquots #4 and #5 to allow for quantification of ferrioxamines by standard addition.
All aliquots were analysed by high performance liquid chromatography – electrospray-ionisation – high resolution mass spectrometry (HPLC-ESI-MS, Ultimate 3000 UHPLC, Q-Exactive ESI-MS, Thermo Scientific). Eluants were (A) 0.1 % formic acid with 5 % methanol and (B) 0.1 % formic acid in methanol[30]. Separation was performed using a 100 × 2.1 mm polystyrene-divinylbenzene column (Hamilton PRP, 5 µm particle size) at a flow rate of 400 µL min^{-1}. A linear gradient of 0 % A to 100 % B over 10 minutes was used and the sample injection volume was 25 µL. For detection by ESI-MS, source conditions were set to an ionisation voltage of +3.5 kV, a capillary temperature of 350°C, a sheath gas flow rate of 35 arbitrary units and an auxiliary gas flow rate of 10 arbitrary units. The heated ion source temperature was set to 300°C. The HPLC flow was diverted to waste during elution of the solvent front (0-0.8 min) and data acquired from 0.8 – 11.8 min. The MS detector acquired data between 275-1500 m/z or 350-1500 m/z in centroid mode. We used an AGC target of 3×10^6 ions and a maximum injection time of 100 ms.

Identification of metallophores

Putative metallophores were identified in aliquots with added Ga from their Ga isotopic signature using Chelomex[24]. Chelomex setting were as follows: relative isotopic ratio for ^{69}Ga:^{71}Ga was set to 0.6±0.1, the relative mass error was set to 2 ppm and the intensity cut off for peaks was 1×10^4 ion counts. A database of $[M\text{-}2H+^{69}Ga]^+$ masses was constructed for putative metallophores identified in +Ga aliquots in all incubations using the software package R[41]. Monoisotopic masses for the ^{56}Fe and Al isotopes were calculated and the mass spectrometry data processing software package MZmine[42] was then used to filter putative metallophores according to the presence/absence of metal complexes in the respective +metal aliquots. Thus positive hits were recorded when Ga complexes were only present in +Ga aliquots and Fe complexes were observed in the +Fe aliquots and exchange of Fe for Ga thus confirmed. MZmine was also used to determine peak areas corresponding to ^{69}Ga, ^{71}Ga, ^{56}Fe and ^{27}Al isotopes in all analysed aliquots. We assumed retention time differences between peaks corresponding to different metal complexes would not vary by more than 2 minutes. Settings for mass tolerance, and peak detection cut-off were equivalent to those used for Chelomex . Finally, since the ^{54}Fe isotope was often too low to detect using our settings in MZmine, extracted mass chromatograms and mass spectra of the Fe metallophores were examined in Xcalibur© (Thermo Scientific) to confirm the presence of the corresponding ^{54}Fe isotope.

Sum formula prediction

We used the accurate mass obtained for Al complexes of our novel metallophores at a nominal resolution of 140,000 ppm (at m/z = 200) to calculate the monoisotopic mass. Based on a lack of detectable adducts, we assumed the metallophores were ionised as $[M\text{-}2H+Al]^+$. The monoisotopic mass was then used in combination with ^{12}C:^{13}C isotopic ratios obtained from averaged mass spectra (n>10) to predict putative sum formulas within 3 ppm of our calculated monoisotopic masses using the Seven Golden Rules[43]. We assumed only carbon, nitrogen, sulphur and hydrogen occurred in our metallophores and further applied reported selection rules with respect to double bond equivalents (DBE must be an integer >0) and the relationship between DBE and O to eliminate unlikely sum formulas[33]. Mass spectra of sum formulas predicted to contain S were checked for observed and predicted abundance of the $^{12}C^{34}S$ isotope to further support or eliminate S content.

Analysis of metallophores in surface seawater samples

For ambient seawater samples, 1 L seawater was directly subsampled from the 20 L high density polyethylene plastic containers and filtered (0.2 µm, 25 mm PVDF sterile syringe filters, Millex®GV) into polycarbonate flasks (Nalgene). Samples were immediately preconcentrated at ambient seawater pH within 2 hours of sampling and processed as for preconcentration of metallophores from incubations.

Statistical approach

Since we were unable to carry out biological replicates for all but one of our experiments, and the biomass we were able to collect for each experiment varied considerably, we cross correlated metallophore abundance with bacterial and Trichome numbers across all our treatments and experiments (n=13), using the R package corrplot[44]. Clustering was carried out according to the hclust function in R using the complete linkage method.

Results and Discussion

Identification of metallophores associated with *Trichodesmium* colonies

M/z [M-2H+Fe]$^{+a}$	Retention time (mins)	Identity/ Predicted formula [M]	Δppm
343.9938 (290.08)	1.5	$C_{11}H_{14}N_2O_8$	0.1
408.0841 (354.16)	1.9	$C_{14}H_{22}N_6O_5$	0.5
435.0952 (381.18)	1.8	$C_{15}H_{23}N_7O_5$	0.9
436.079 (382.16)	1.9	$C_{15}H_{22}N_6O_6$	0.4
450.0584 (396.14)	2.5	$C_{15}H_{20}N_6O_7$	0.7
526.0811 (472.16)	6.9		
538.1001 (484.14)	4.6	$C_{21}H_{24}N_8O_6$	0.1
542.0585 (488.14)	1.5	$C_{19}H_{20}N_8O_8$	1.2
614.273 (560.35)	5.1	desferrioxamine B, $C_{25}H_{48}N_6O_8$	1.5
620.1026 (566.18)	4.0	$C_{23}H_{34}O_{16}$	1.3
654.2676 (600.35)	6.8	desferrioxamine E, $C_{27}H_{48}N_6O_9$	0.9
672.2785 (618.36)	5.4	desferrioxamine G, $C_{27}H_{50}N_6O_{10}$	1.4
678.257 (624.34)	4.5	$C_{30}H_{48}N_4O_{10}$	0.3
684.120 (630.2)	1.1		
720.2527 (666.33)	2.0	$C_{29}H_{46}N_8O_{10}$	0.4
726.2285 (672.31)	1.9	$C_{35}H_{48}N_2O_9S$	2.4
753.2396 (699.32)	4.6	$C_{33}H_{45}N_7O_{10}$	2.6
780.2509 (726.33)	1.8		

We undertook four incubation experiments in the Gulf of Aqaba in the spring of 2016 (April 20, May 01, May 02) and 2017 (May 07) to identify metallophores associated with natural *Trichodesmium* colonies. We used the distinctive isotopic signatures of Ga and Fe to identify 18 compounds that occurred in our incubations (Table 1, Fig. S2). The metallophores were not present in the filtered seawater used in the incubations (Fig. 1). We also tested the supernatant of stationary phase *Trichodesmium erythraeum* IMS101 filaments grown in culture and did not observe any of these metallophores (Fig. S3). We therefore conclude that the metallophores identified here are specifically associated with harvested natural *Trichodesmium* colonies and may thus be produced as a result of colony formation and/or microbiome composition.

Table 1. Mass to charge ratios (m/z), retention time and predicted sum formula or identity of the Fe complexes for metallophores identified in incubations of Trichodesmium erythraeum tuft-shaped colonies. Also provided is the difference between observed and predicted sum formula (Δppm).

As recently reported, three of the compounds were identified as well-known siderophores ferrioxamines B, G and E (FOB, FOG and FOE)[17]. However, fifteen of the metallophores associated with natural *Trichodesmium* colonies had mass to charge ratios that do not correspond with known siderophores. We used rigorous MIP identification criteria that required exchange between Fe and Ga, and the identification of the isotopic signatures of both metals, as a prerequisite for a positive metallophore identification[23,31]. Our criteria reduced a possible 127 hits obtained for the Ga isotopic signature alone to the final list of eighteen compounds exhibiting both Fe and Ga isotopic patterns. The applied criteria reduced the likelihood of false positives but likely excluded some compounds with ^{54}Fe isotopic signatures too low to detect. The number and diversity of metallophores detected in these incubations is thus a conservative estimate of the number of compounds associated with *Trichodesmium* colonies that are capable of binding metals.

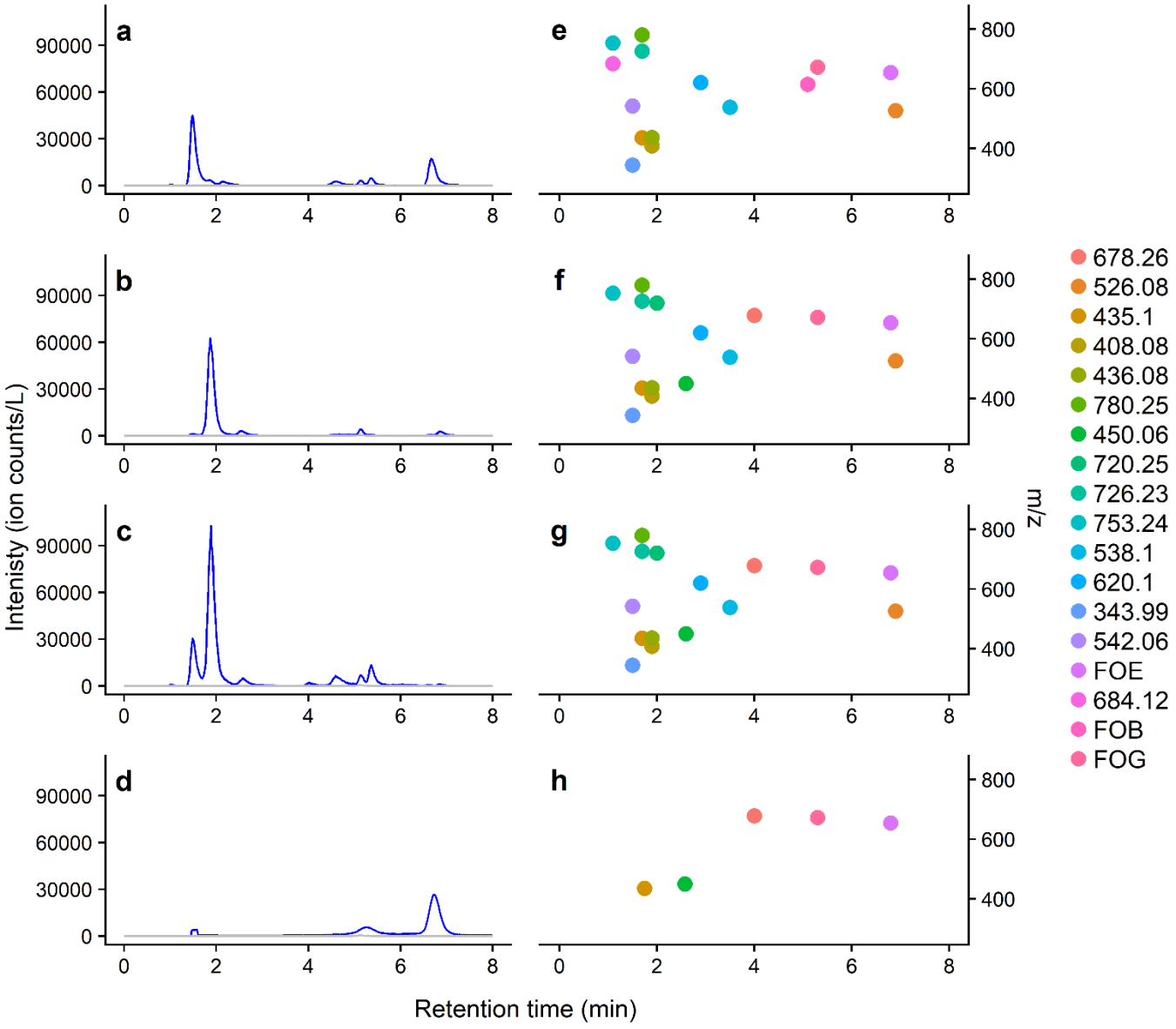

Figure 1 - Sum of extracted ion chromatograms (a-d) for Fe complexes of all metallophores identified in aliquots after addition of Fe, after normalisation to the volume of seawater extracted. The grey line is the extracted ion chromatogram obtained for filtered seawater prior to addition of colonies. (e-h) shows retention times of metallophores as a function of mass:charge ratio (m/z). From top to bottom, panels show data obtained for the initial time point in experiments undertaken on (a, e) April 20 (GoA-1), (b, f) May 1 (GoA-2a), (c, g) May 2 (GoA-2b) in 2016 and (d, h) May 7, 2017 (GoA-3).

All but one of the novel metallophores eluted earlier than the ferrioxamine siderophores, suggesting they were hydrophilic in nature (Table 1, Fig. 1). Our novel metallophores have similar retention times to Fe (III) rhodotoluate, which is a charged siderophore at low pH[22] but are much more hydrophilic than marine siderophores with fatty acid chains such as the amphibactins, which are well retained during reverse phase chromatography[31,45]. Extracted ion chromatograms (examples shown in Fig 1a-d) showed that the cumulative sum of the ions eluting at 1.5 and 1.9 min resulted in the two most intense peaks. Although some metallophores co-eluted at 1.5, 1.8 and 1.9 min, the differences in m/z were not consistent with commonly observed adducts[46] and so these metallophores were assumed to be distinct. Comparison of ion counts after normalisation to extraction volume (Fig 1e-g) showed that the compound with m/z = 720.251 produced the highest ion counts overall, although this is not necessarily a reflection of higher concentrations, since ESI-MS ionisation efficiencies differ considerably from ion to ion.

Our method for sum formula prediction allowed us to assign formulas to all but three of the novel metallophores (m/z = 526.081, 684.120, 780.251, Table 1). Predicted sum formulas were rich in oxygen, which is expected for high affinity Fe(III) binding compounds. Although sum formulas with one or two sulphur atoms were predicted for some metallophores (e.g. m/z =408.084, 538.100, 684.120, 726.229), sulphur content for all but m/z = 726.229 were ruled out based on closer examination of observed and predicted abundance of the $^{12}C^{34}S$ isotope. Sum formulas fell within the van Krevelen space occupied by known siderophores[28] (Fig. 2a), which provides confidence in

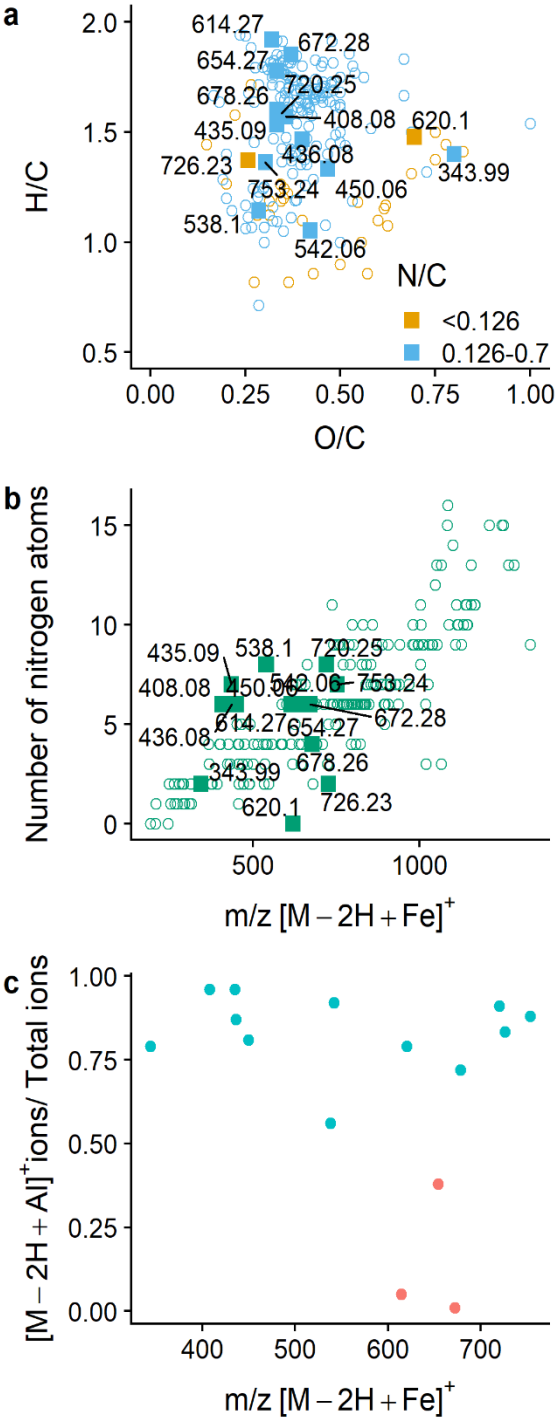

Figure 2 - Characterisation of metallophores associated with *Trichodesmium* colonies a) Van Krevelen diagram of predicted sum formulas for ferrioxamine siderophores and novel metallophores identified in this study (solid squares). Open circles are van Krevelen characteristics obtained for a database of known siderophores. b) Predicted number of N atoms as a function of m/z of the Fe(III) complex. Filled squares are metallophores identified in this study, open circles are for known siderophores. c) Ratio of peak areas for the Al complexes to the sum of Fe+Al complexes in the presence of 10^5 excess Al. Ferrioxamine B,E and G are red and novel metallophores are blue.

our predictions. Increasing number of N along with an increased molecular weight suggests a type of metallophores with a peptide backbone[28]. However, sum formulas for all but one of our metallophores with m/z<550 were relatively nitrogen rich in comparison with known siderophores (Fig. 2b).

Furthermore, two of our metallophores were predicted to have N/C ratios less than those typical for peptides and proteins[47], with one compound (m/z 620.103) predicted to contain no nitrogen. Low N/C ratios are observed in a limited number of characterised catecholate and carboxylate type siderophores (Fig. 2a), however m/z 620.103 was clearly unlikely to be derived from amino acids.

The specificity of pathways employed to synthesize siderophores can result in families of siderophores with the same peptide sequence[48,49] and thus the same number of N atoms. It is possible that sum formulas with similar numbers of N atoms are therefore structurally related. We observed that three of our novel metallophores contained 6 N atoms but differed in m/z ratio by a single ethyl or carbonyl group (m/z = 408.084, 436.079 and 450.058). However, we were unable to collect enough MS^2 data to support any structural relationship between these metallophores. The remaining novel metallophores could not be related to each other via addition or removal of simple functional groups.

The detection of the unknown Fe and Ga complexes at low pH (samples were stored and analysed at pH<3) suggests that these metallophores have a high affinity for hard trivalent metals. For example, the known ferrioxamine siderophores detected here have log affinity constants > 30 for Fe in aqueous solutions[50]. In support of this, we noted that Al complexes were also observed in our chromatograms for many of our metallophores, likely attributable to the presence of background Al in our samples. We confirmed complexation of Al through addition of ca. 10^5 fold excess of aluminium (final concentration 1 mmol L^{-1}) to our extracts, which resulted in increased abundance for all putative Al complexes. However, even in the presence of excess Al, ion counts for Al complexes of FOB, FOE and FOG only constituted 5 ± 6 %, 38 ± 35 %, and 2 ± 6 % (n=13) of the summed ion counts for Al and Fe complexes, respectively (Fig 2c), reflecting the very high affinity of these primary siderophores for Fe compared to other trivalent metals[49,51]. In contrast Al complexes made up the major portion of all complexes for the other identified metallophores, since Al ion counts constituted between 66 and 98 % of the summed (Fe+Al) ion counts. We therefore suggest that our novel metallophores had a lower relatively affinity for Fe than ferrioxamines.

Metallophores in incubations of *Trichodesmium* colonies

Our incubations contained different quantities of *Trichodesmium* colonies and associated bacteria as a result of variability in the natural abundance of *Trichodesmium* in the GoA at the time of sampling. In April-May of 2016 a large bloom of *Trichodesmium* tuft-shaped colonies occurred with a peak in abundance on May 2nd (Fig. S1, Table S1). High colony abundance in May 2016 allowed us to collect and incubate up to 15 × 10^5 trichomes L^{-1} for our GoA-2 experiments, whilst the lower abundance of *Trichodesmium* in May 2017 meant that GoA-3 incubations started with only 0.17 × 10^5 trichomes L^{-1} (Fig. 3a). Numbers of colony associated bacteria also varied between incubations but did not correlate with *Trichodesmium* (r =0.32, p>0.05), with highest initial bacterial counts observed

in the GoA-2b experiments (Fig. 3b). For GoA-1, 2a and 3, trichome abundances were relatively stable over the course of the 24-hour incubation, whilst bacterial numbers increased. GoA-2b was different from the other incubations in that both trichome and bacterial numbers decreased over the course of the incubation, by 30 and 60 % respectively.

Along with variability in the relative contribution of host versus

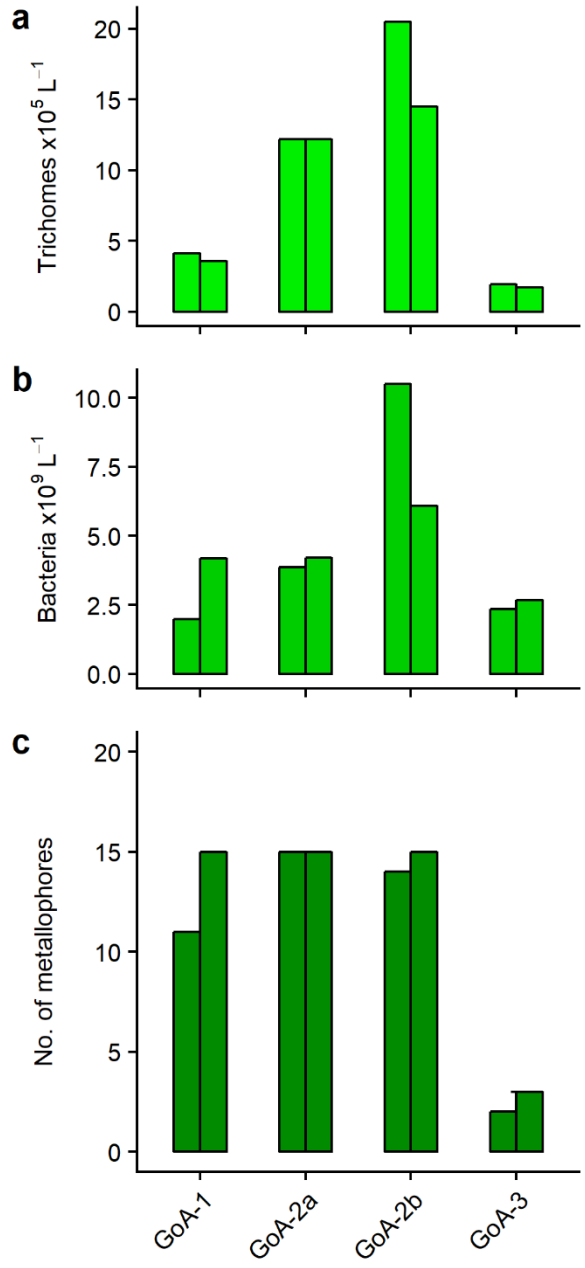

Figure 3 - Abundance of trichomes (a), bacteria (a) and number of metallophores (c) observed at the beginning of incubations (left bars) and after 1 day (right bars) in incubations of natural *Trichodesmium erythraeum* tuft-shaped colonies in filtered sterilised metallophore free seawater. GoA-1 – 3 correspond to incubation experiment dates (see Methods for details).

associated bacteria, we observed some variability in the number of metallophores identified in the incubations. Maximum diversity was associated with the bloom of *Trichodesmium erythraeum* that occurred in April-May 2016 (GoA-1, GoA-2), and lower numbers of metallophores (3) were observed in the incubations in May 2017 (GoA-3). The variability in metallophore diversity was likely related to *Trichodesmium* abundance in the incubations, since biomass was also lower in May 2017 than in April and May 2016. The number of metallophores either remained the same or increased slightly over the course of the incubations. We also observed highest overall ion counts for many of the detected masses in GoA-2b (Fig. 1, Table S2). Thus, the abundance of the metallophores was also highest in incubations with the highest number of *Trichodesmium* colonies. We cross-correlated normalised metallophore abundance, trichome and bacterial numbers observed in all our experiments and treatments (n = 13 for each parameter) in order to examine relationships between the metallophores and bulk constituents of the colony consortium. Absolute quantification of unknown siderophores is not possible with ESI-MS. Indeed, even our approach of using variations in relative abundances between samples must be treated with caution, since ion response can vary from sample to sample depending on the presence of other compounds. However, we quantified our ferrioxamine siderophores by standard addition and observed that the ESI-MS response for ferrioxamine B was reasonably consistent across our samples (average response for FOB = $2.0\pm1.5\times10^6$ ion counts fmol^{-1}, n=13). Thus, we think it unlikely that ion responses were influenced too strongly by changes in organic matter composition between incubations.

Hierarchical clustering of the resultant correlation matrix (Fig. S4) suggested that our metallophores fell into three groups. The largest group designated “Group A” and shown in blue on the x-axis in Figure 4, contained 10 of our novel metallophores, and compounds in this group significantly correlated with *Trichodesmium* abundance ($r>0.56$, $p<0.05$, Fig. S4). A dominant driver behind the occurrence of Group A was the high abundance of *Trichodesmium* in the May 2016 experiments. Interestingly, the three novel metallophores with 6 N (m/z = 408.084, 436.079 and 450.058) all fell into this group and strongly correlated with each other ($r>0.92$, $p<0.001$, Fig. S4). Furthermore, we noted a weak negative correlation between six of the novel metallophores in Group A and ferrioxamine E ($r<-0.56$, $p<0.05$). A second group designated “Group B” (red on the x-axis in Fig. 4), contained metallophores with m/z 343.994, 538.100, 542.059, and 620.103 and did not significantly correlate with abundances of bacteria or *Trichodesmium*. We note that this group incorporated the two metallophores with predicted sum formulas with low or no nitrogen (m/z =343.99, 620.10; Table 1). Although neither group A or B correlated with overall bacterial numbers, we do not rule out a bacterial source, since total bacterial numbers may not be representative of variability in or activity of individual members of the population. Our final group (purple on the x-axis in Fig. 4) included the three ferrioxamine siderophores and the last novel

metallophore (m/z = 684.120). We found that FOB and FOG correlated weakly with bacterial numbers (r = 0.66 and 0.59, n=13, p<0.05, Fig. S4), and that FOE correlated with FOB and FOG (r>0.83, p<0.001). The novel metallophore m/z = 684.12 minimal carry over of ambient seawater associated with the *Trichodesmium* colonies via washing of colonies in FSW prior to the start of the incubations. Thus, we argue that the high abundance of many of our novel metallophores within 2 hours

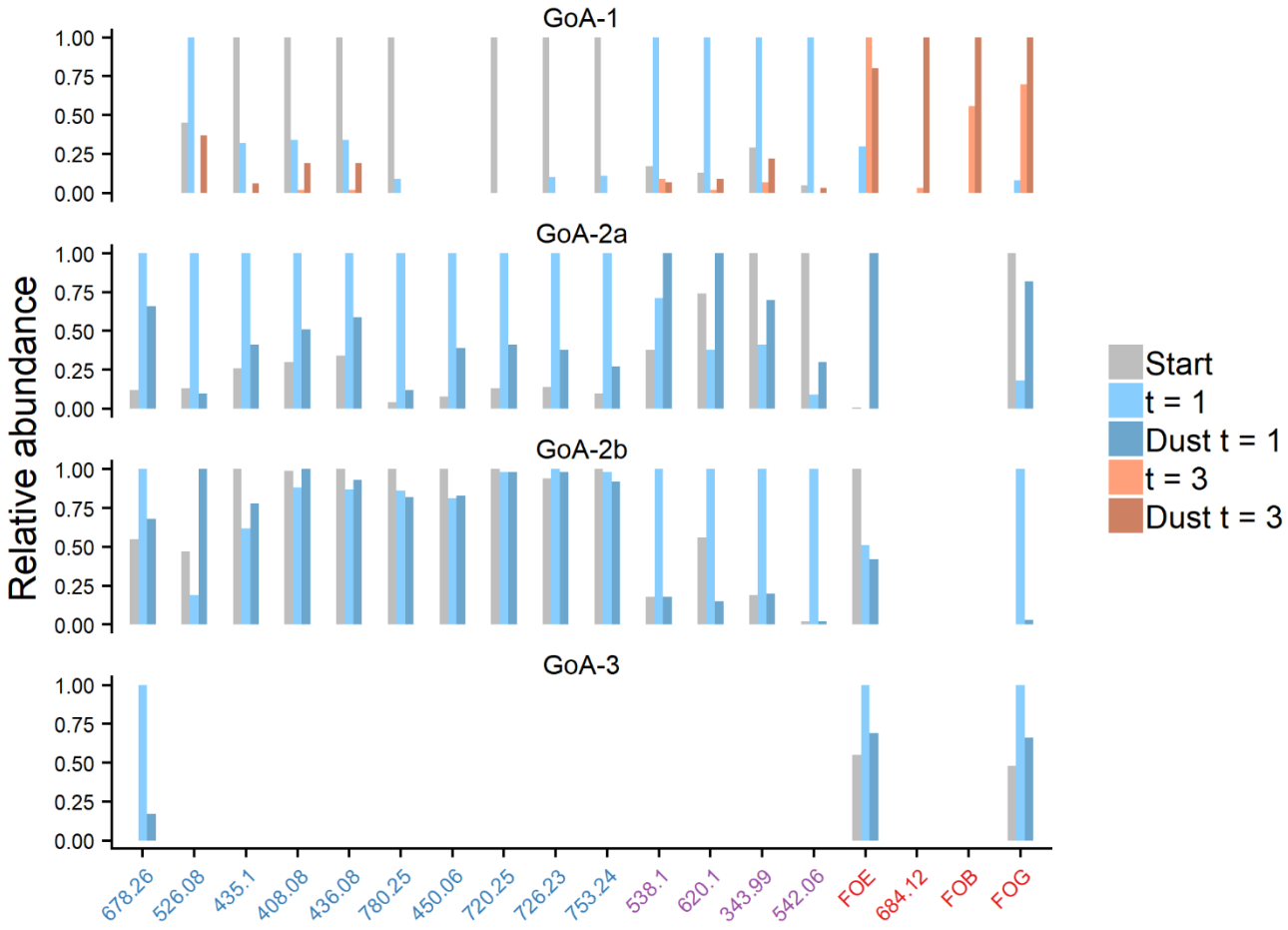

Figure 4. Normalised metallophore abundance in *Trichodesmium* incubations at the start of the incubations, after 1 day (t=1) and 3 days (t=3, GoA-1 only) after addition to metallophore free, sterilized, filtered seawater. Abundance of each metallophore was normalized to the maximum observed for that metallophore within each experiment. Metallophore identity (see Table 1) is given on the y axis, and text colour indicates clusters of correlating metallophores. Blue metallophores (Group A) clustered with *Trichodesmium* biomass, red metallophores (Group B) with each other and purple metallophore (FOX group) with bacteria. GoA-1 – 3 correspond to incubation experiments undertaken on separate dates (see Methods for details).

correlated more strongly with bacterial numbers (r=0.79, p<0.01), FOB and FOG (r>0.81, p<0.001). Since all three of the ferrioxamine siderophores fell into this group, we designate this group the FOX group. The clustering of this group with bacterial numbers is consistent with a heterotrophic bacterial source for the FOX group, and indeed we successfully isolated a ferrioxamine E producing bacteria from our *Trichodesmium* colonies[17].

We further examined the impact of incubation conditions (time, added dust) on the abundance of our metallophore groups in an effort to better understand the factors influencing their distributions. We examined changes in metallophore abundance over a period of 72 hours in GoA-1, and at the beginning and after 24 hours in the remaining GoA experiments. Overall the behaviour of the metallophores with incubation time was somewhat variable (Fig. 4). However, it was apparent that many of the novel metallophores were relatively abundant even at the first sampling time point, which occurred within two hours of adding *Trichodesmium* tuft-shaped colonies to the metallophore-free FSW. Care was taken to try to ensure of adding *Trichodesmium* colonies in the GoA-2b experiment was mostly due to release of the metallophores from the very high number of colonies we were able collect in this experiment (Fig. 3), although carry over of some metallophores along with ambient seawater cannot be entirely ruled out. Furthermore, we suspect the bloom from which these colonies were sampled was in its final stages, since we observed a rapid subsequent decline in *Trichodesmium* at the sampling site. Previous work has shown that release of EPS, which may also incorporate metallophores[20,21], is associated with bloom termination and nutrient stress[18,19].

Subsequent variability in metallophores is likely then driven by the complex interactions amongst the microbial consortium during the course of the incubations. For example, in the April 2016 experiment (GoA-1), we observed a decrease in Group A metallophores over the course of the incubation. In contrast, FOX metallophores were not detected at the start of the experiment but increased with time so that all FOX metallophores were detectable after 24 hours of incubation and further increased over the subsequent 48 hours (Fig. 4).

Quantification of the three ferrioxamine siderophores showed that the final concentration of the sum of ferrioxamine B, E and G came to 1.0 nmol L^{-1} after 72 hours of incubation, with ferrioxamine E and G making up 90% of the total[17]. In this case the increase in the FOX group was consistent with observed increases in bacterial numbers and it is this experiment which largely drives the clustering of bacterial numbers with the FOX group of metallophores and the weak negative correlation between the FOX group and some Group A metallophores.

Experiments undertaken a month later in May 2016 (GoA-2a) resulted in increases in all group A metallophores over the 24 hour incubation period, whilst incubations started with fresh *Trichodesmium* colonies just a day later for GoA-2b resulted in no change in Group A metallophores, possibly because abundance was already high at the start of these incubations. The responses of the metallophores are potentially linked to a number of factors related to the natural variability of the harvested colonies that were sampled at different time points in the evolution of the *Trichodesmium* bloom. Previous work has shown variability in both Fe uptake rates and mineral Fe availability for natural *Trichodesmium* colonies sampled at separate time points[11,12,17]. In addition, both associated bacterial community composition and bacterial numbers are also likely to vary considerably dependent on the phase of the *Trichodesmium* bloom, the health of the colonies and the sampling location[13,14,52]. Such variability was observed in our experiments, where the response of bacteria to the incubation conditions was strongest for the GoA-1 experiment[17] and where the longer timescale of the incubation may have been favourable for associated copiotrophic bacteria. In contrast, we observed a decline in both Trichomes and bacterial numbers in the GoA-2b incubations, which corresponded with a reduction in the FOX group metallophores, but not group A or B metallophores, and which we suspect was due to a more advanced state of the *Trichodesmium* bloom sampled on this day.

Addition of atmospherically derived dust to the incubations had a variable impact on metallophore abundance. As we have reported earlier, dust appeared to have a positive effect on FOX group metallophores in GoA-1 and GoA-2a[17] which we attribute to the ability of copiotrophic bacteria to respond to favourable conditions and increase production of FOX metallophores within the timescale of our experiments. However, for the remaining metallophores, no consistent effects of dust were observed, and further work is required to fully assess the role these compounds might play in interactions between the *Trichodesmium* and mineral dust trapped within the colony environment.

Occurrence of metallophores in filtered surface seawater samples

We determined metallophore abundance in filtered surface seawater samples in the Gulf of Aqaba at the peak of the *Trichodesmium* bloom (May 2nd 2016), and in three replicate samples collected in February 2017 (Table 2) when *Trichodesmium* colonies were absent. We detected 16 out of 18 of the metallophores in our May 2016 sample, which was collected at the same time as we started our GoA-2b incubations, but only 3 metallophores in Feb 2017 when *Trichodesmium* was not present in the Gulf of Aqaba. Group A and B metallophores were thus all present in our filtered surface seawater sample at the peak of the May 2016 *Trichodesmium erythraeum* bloom. Whilst of limited extent, our observations of metallophore abundance in filtered surface seawater samples are thus consistent with our incubation results and further support the association of Group A and B metallophores with *Trichodesmium* tuft-shaped colonies. In contrast, three of the FOX group siderophores were either absent (FOB and the novel metallophore m/z = 684.12), or present at lower concentrations in May 2016 (FOG) compared to February 2017. Ferrioxamine E was observed at similar concentrations in May 2016 and in Feb 2017. Since ferrioxamines E and G were present at a time when *Trichodesmium* was absent, the occurrence of these siderophores in surface waters of the GoA was not related to *Trichodesmium* abundance. This finding is consistent with previous findings that the ferrioxamine siderophores are common in surface waters[30,45,53,54], even in regions where Fe concentrations are not sufficiently low to limit phytoplankton growth[55] such as the Gulf of Aqaba. Concentrations of ferrioxamine E detected in our study are higher than those reported previously[30,45,53], although our results are consistent with other studies suggesting production of ferrioxamines by copiotrophic bacteria capable of rapidly exploiting carbon sources[53,56].

Table 2. Metallophores identified in ambient surface seawater samples collected in the Gulf of Aqaba on May 02, 2016 at a time of high *Trichodesmium* abundance and on Feb 07, 2017 (n =3) when *Trichodesmium* was not detected. Metallophore identities are given in Table 1. Ferrioxamine siderophores were quantified and expressed as concentrations in the ambient seawater after accounting for preconcentration factors, but not preconcentration efficiency. Metallophores newly identified in this study are donated as "Present" or "Not detected", since they could not be quantified.

Metallophore identity	May 2nd 2016	Feb 7th 2017
678.26	Present	Not detected
526.08	Present	Not detected
435.10	Present	Not detected
408.08	Present	Not detected
436.08	Present	Not detected
780.25	Present	Not detected
450.06	Present	Not detected
720.25	Present	Not detected
726.23	Present	Not detected
753.24	Present	Not detected
538.1	Present	Not detected
620.1	Present	Not detected
343.99	Present	Not detected
542.06	Present	Not detected
FOE	42 pmol L^{-1}	41 ± 19 pmol L^{-1}
684.12	Not detected	Not detected
FOB	Not detected	2.1 pmol L^{-1} (n=1)
FOG	1.4 pmol L^{-1}	18 ± 8 pmol L^{-1}

Conclusions

For the first time, we have identified a total of 18 metallophores associated with natural tuft-shaped colonies of *Trichodesmium erythraeum*. Fifteen of our identified metallophores have not, to our knowledge, been previously described, while the remaining metallophores were identified as the well-known siderophores ferrioxamine B, E and G.

We used multiple strands of evidence to investigate the source and character of the novel metallophores. The apparent hydrophilicity, nitrogen content of predicted sum formulas and affinity for Al suggests that the novel metallophores described here are unlike previously described marine siderophores. *Trichodesmium* colonies *in situ* and in incubations produced and released multiple unconnected metallophores that are capable of binding with trivalent metals other than Fe. The variability in sum formulas suggests that our novel metallophores are unlikely to be synthesized by a single metabolic pathway, and furthermore may not be produced by a single microbe within the colony consortium. Nevertheless ten out of our 15 novel metallophores correlated with *Trichodesmium* filament abundance and we argue that these metallophores are likely to have a more specific association with *Trichodesmium*, although we found no evidence of these metallophores in our *Trichodesmium erythraeum* IMS 101 cultures. Since our IMS101 cultures were comprised of filaments, it is possible that colony formation is important for production of these metallophores. Production via microbial remineralisation of e.g. EPS is possible but unlikely for all of the novel metallophores, since 13 out of 15 are nitrogen rich and organic carbon generally becomes nitrogen deplete as it is remineralised[57].

In contrast to our novel metallophores, the abundance of the ferrioxamine siderophores B, G and E was not linked strongly to *Trichodesmium*, and we therefore suggest that the production of these three siderophores in both our incubations and in the ambient seawater could result from the ubiquitous presence of ferrioxamine producing copiotrophic bacteria[13,14,56,58]. These bacteria likely opportunistically attach to *Trichodesmium* and benefit from the carbon and nitrogen produced by *Trichodesmium* colonies. However, since we have also shown that these siderophores influence Fe dissolution and Fe uptake rates observed in *Trichodesmium* colonies[17], we suggest that these bacteria nevertheless have the potential to engage in Fe-for-C/N trading within the colony environment.

We conclude that the *Trichodesmium* colony microbiome supports a distinctive "ligandosphere" a term recently proposed by Deicke et al., 2019[33] to describe the entirety of excreted metal complexing agents and ligands derived from dissolved organic matter within a microbial environment. The association of this "ligandosphere" with *Trichodesmium* colonies might be expected to have consequences for solubilisation of Fe from atmospheric dust captured by the colony and suggests organic matter associated with *Trichodesmium* colonies can modify metal speciation with potential consequences for metal availability. In this regard the formation of Al complexes is particularly interesting given that Al can contribute 2 % by weight of mineral dust[10] and is typically present at higher concentrations relative to Fe in surface seawater influenced by dust deposition[38]. Production of distinct suites of metallophores by different components of the colony consortium also raises the potential that these compounds are important for nutrient trade-offs and our work suggests that these metallophores will impact on utilisation of dust as a source of nutrients. Further work is required to further characterise and understand the environmental variability of these metallophores, and their relationship to the potential for *Trichodesmium* to exploit niche environments and thereby contribute to the ocean's nitrogen inventory.

Conflicts of interest

There are no conflicts to declare.

Acknowledgements

The authors would like to thank the reviewers for their constructive comments on the manuscript. This work was funded by the German-Israeli Foundation for Scientific Research and Development (Grant 1349), the Helmholtz Association and the Israel Science Foundation (Grant 458/15). The authors would like to thank M. Seidel for advice on sum formula assignments.

References

1 D. G. Capone, J. P. Zehr, H. W. Paerl, B. Bergman and E. J. Carpenter, *Science (80-.).*, 1997, **276**, 1221–1229.

2 D. G. Capone, J. A. Burns, J. P. Montoya, A. Subramaniam, C. Mahaffey, T. Gunderson, A. F. Michaels and E. J. Carpenter, *Global Biogeochem. Cycles*, 2005, **19**, GB2024.

3 B. Bergman, G. Sandh, S. Lin, J. Larsson and E. J. Carpenter, *FEMS Microbiol. Rev.*, 2013, **37**, 286–302.

4 A. Kustka, S. Sañudo-Wilhelmy, E. J. Carpenter, D. G. Capone and J. A. Raven, *J. Phycol.*, 2003, **39**, 12–25.

5 C. M. Moore, M. M. Mills, K. R. Arrigo, I. Berman-Frank, L. Bopp, P. W. Boyd, E. D. Galbraith, R. J. Geider, C. Guieu, S. L. Jaccard, T. D. Jickells, J. La Roche, T. M. Lenton, N. M. Mahowald, E. Maranon, I. Marinov, J. K. Moore, T. Nakatsuka, A. Oschlies, M. A. Saito, T. F. Thingstad, A. Tsuda and O. Ulloa, *Nat. Geosci.*, 2013, **6**, 701–710.

6 M. Rubin, I. Berman-Frank and Y. Shaked, *Nat. Geosci.*, 2011, **4**, 529–534.

7 S. Richier, A. I. Macey, N. J. Pratt, D. J. Honey, C. M. Moore and T. S. Bibby, *PLoS One*, 2012, **7**, e35571.

8 B. A. S. Van Mooy, L. R. Hmelo, L. E. Sofen, S. R. Campagna, A. L. May, S. T. Dyhrman, A. Heithoff, E. A. Webb, L. Momper and T. J. Mincer, *ISME J*, 2012, **6**, 422–429.

9 T. Jickells and C. M. Moore, *Annu. Rev. Ecol. Evol. Syst.*, 2015, **46**, 481–501.

10 N. M. Mahowald, D. S. Hamilton, K. R. M. Mackey, J. K. Moore, A. R. Baker, R. A. Scanza and Y. Zhang, *Nat. Commun.*, 2018, **9**, 2614.

11 S. Basu and Y. Shaked, *Limnol. Oceanogr.*, 2018, **63**, 2307–

2320.
12 M. Eichner, S. Basu, M. Gledhill, D. de Beer and Y. Shaked, *Front. Microbiol.*, 2019, **10**, 1565.
13 M. D. Lee, N. G. Walworth, E. L. McParland, F.-X. Fu, T. J. Mincer, N. M. Levine, D. A. Hutchins and E. A. Webb, *ISME J.*, 2017, **11**, 1813–1824.
14 K. R. Frischkorn, M. Rouco, B. A. S. Van Mooy and S. T. Dyhrman, *ISME J.*, 2017, **11**, 2090–2101.
15 S. Basu, M. Gledhill, D. de Beer, S. P. Matondkar and Y. Shaked, *Commun. Biol.*, 2019, **2**, 284.
16 R. Hermenau, K. Ishida, S. Gama, B. Hoffmann, M. Pfeifer-Leeg, W. Plass, J. F. Mohr, T. Wichard, H.-P. Saluz and C. Hertweck, *Nat. Chem. Biol.*, 2018, **14**, 841–843.
17 S. Basu, M. Gledhill, D. de Beer, S. P. Matondkar and Y. Shaked, *Commun. Biol.*
18 E. Bar-Zeev, I. Avishay, K. D. Bidle and I. Berman-Frank, *ISME J.*, 2013, **7**, 2340–2348.
19 I. Berman-Frank, G. Rosenberg, O. Levitan, L. Haramaty and X. Mari, *Env. Microbiol*, 2007, **9**, 1415–1422.
20 C. S. Hassler, V. Schoemann, C. M. Nichols, E. C. V Butler and P. W. Boyd, *Proc. Natl. Acad. Sci. U. S. A.*, 2011, **108**, 1076–1081.
21 C. S. Hassler, E. Alasonati, C. A. M. Nichols and V. I. Slaveykova, *Mar. Chem.*, 2011, **123**, 88–98.
22 P. McCormack, P. J. Worsfold and M. Gledhill, *Anal. Chem.*, 2003, **75**, 2647–2652.
23 M. Deicke, J. F. Mohr, J.-P. Bellenger and T. Wichard, *Analyst*, 2014, **139**, 6096–6099.
24 O. Baars, F. M. M. Morel and D. H. Perlman, *Anal. Chem.*, 2014, **86**, 11298–11305.
25 R. M. Boiteau, J. N. Fitzsimmons, D. J. Repeta and E. A. Boyle, *Anal. Chem.*, 2013, **85**, 4357–4362.
26 M. Gledhill, P. McCormack, S. Ussher, E. P. Achterberg, R. F. C. Mantoura and P. J. Worsfold, *Mar. Chem.*, 2004, **88**, 75–83.
27 S. M. Lehner, L. Atanasova, N. K. N. Neumann, R. Krska, M. Lemmens, I. S. Druzhinina and R. Schuhmacher, *Appl. Environ. Microbiol.*, 2013, **79**, 18–31.
28 T. Pluhacek, K. Lemr, D. Ghosh, D. Milde, R. Novak and V. Havlícek, *Mass Spectrom. Rev.*, 2016, **35**, 35–47.
29 M. Deicke, J.-P. Bellenger and T. Wichard, *J. Chromatogr. A*, 2013, **1298**, 50–60.
30 E. Mawji, M. Gledhill, J. A. Milton, G. A. Tarran, S. Ussher, A. Thompson, G. A. Wolff, P. J. Worsfold and E. P. Achterberg, *Environ. Sci. Technol.*, 2008, **42**, 8675–8680.
31 E. Mawji, M. Gledhill, J. A. Milton, M. V Zubkov, A. Thompson, G. A. Wolff and E. P. Achterberg, *Mar. Chem.*, 2011, **124**, 90–99.
32 T. Wichard, *Front. Mar. Sci.*, 2016, **3**, 131.
33 M. Deicke, J. F. Mohr, S. Roy, P. Herzsprung, J.-P. Bellenger and T. Wichard, *Metallomics*, 2019, **11**, 810–821.
34 O. Baars, X. Zhang, F. M. M. Morel and M. R. Seyedsayamdost, *Appl. Environ. Microbiol.*, , DOI:10.1128/aem.03160-15.
35 R. M. Boiteau, S. J. Fansler, Y. Farris, J. B. Shaw, D. W. Koppenaal, L. Pasa-Tolic and J. K. Jansson, *Metallomics*, 2019, **11**, 166–175.
36 A. M. L. Kraepiel, J. P. Bellenger, T. Wichard and F. M. M. Morel, *BioMetals*, 2009, **22**, 573–581.
37 S. M. Kraemer, O. W. Duckworth, J. M. Harrington and W. D. C. Schenkeveld, *Aquat. Geochemistry*, 2015, **21**, 159–195.
38 J.-L. Menzel Barraqueta, J. K. Klar, M. Gledhill, C. Schlosser, R. Shelley, H. F. Planquette, B. Wenzel, G. Sarthou and E. P. Achterberg, *Biogeosciences*, 2019, **16**, 1525–1542.
39 A. Torfstein, N. Teutsch, O. Tirosh, Y. Shaked, T. Rivlin, A. Zipori, M. Stein, B. Lazar and Y. Erel, *Geochim. Cosmochim. Acta*, 2017, **211**, 373–393.
40 W. G. Sunda, N. M. Price and F. M. M. Morel, in *Algal Culturing Techniques*, ed. R. A. Anderson, Elsevier, 2005, pp. 35–65.
41 R Development Core Team, *R Found. Stat. Comput. Vienna Austria*, 2016, {ISBN} 3-900051-07-0.
42 T. Pluskal, S. Castillo, A. Villar-Briones and M. Orešič, *BMC Bioinformatics*, 2010, **11**, 1–11.
43 T. Kind and O. Fiehn, *BMC Bioinformatics*, 2007, **8**, 105.
44 T. Wei and V. Simko, 2017.
45 R. M. Boiteau, D. R. Mende, N. J. Hawco, M. R. McIlvin, J. N. Fitzsimmons, M. A. Saito, P. N. Sedwick, E. F. DeLong and D. J. Repeta, *Proc. Natl. Acad. Sci. U. S. A.*, 2016, **113**, 14237–14242.
46 N. Huang, M. M. Siegel, G. H. Kruppa and F. H. Laukien, *J. Am. Soc. Mass Spectrom.*, 1999, **10**, 1166–1173.
47 A. Rivas-Ubach, Y. Liu, T. S. Bianchi, N. Tolić, C. Jansson and L. Paša-Tolić, *Anal. Chem.*, 2018, **90**, 6152–6160.
48 J. M. Vraspir and A. Butler, *Ann. Rev. Mar. Sci.*, 2009, **1**, 43–63.
49 R. C. Hider and X. L. Kong, *Nat. Prod. Rep.*, 2010, **27**, 637–657.
50 A. L. Crumbliss, in *CRC Handbook of microbial iron chelates*, ed. G. Winkelmann, CRC Press Ltd, Boca Raton, Florida, 1991, pp. 177–233.
51 T. C. Johnstone and E. M. Nolan, *Dalt. Trans.*, 2015, **44**, 6320–6339.
52 L. R. Hmelo, B. A. S. Van Mooy and T. J. Mincer, *Aquat. Microb. Ecol.*, 2012, **67**, 1–14.
53 R. M. Bundy, R. M. Boiteau, C. McLean, K. A. Turk-Kubo, M. R. McIlvin, M. A. Saito, B. A. S. Van Mooy and D. J. Repeta, *Front. Mar. Sci.*, 2018, **5**, 61.
54 R. M. Boiteau, C. P. Till, T. H. Coale, J. N. Fitzsimmons, K. W. Bruland and D. J. Repeta, *Limnol. Oceanogr.*, 2019, **64**, 376–389.
55 Z. Chase, A. Paytan, K. S. Johnson, J. Street and Y. Chen, *Global Biogeochem. Cycles*, 2006, **20**, GB3017.
56 I. B. Velasquez, E. Ibisanmi, E. W. Maas, P. W. Boyd, S. Nodder and S. G. Sander, *Front. Mar. Sci.*, 2016, **3**, 172.
57 D. A. Hansell, *Ann. Rev. Mar. Sci.*, 2013, **5**, 421–445.
58 R. M. Bundy, D. V. Biller, K. N. Buck, K. W. Bruland and K. A. Barbeau, *Limnol. Oceanogr.*, 2014, **59**, 769–787.